RSC Advances

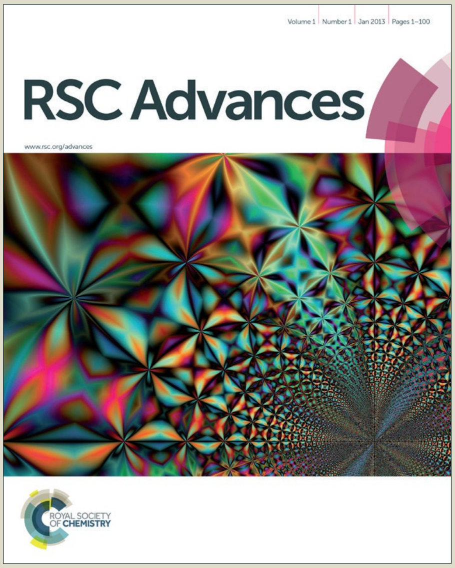

ROYAL SOCIETY
OF CHEMISTRY

www.rsc.org/advances

RSC Advances

ARTICLE

Inkjet Printing of Silver Rainbow Colloids for SERS Chips with Polychromatic Sensitivity

Received 00th January 20xx,
Accepted 00th January 20xx

DOI: 10.1039/x0xx00000x

www.rsc.org/

K. E. Yorov,[a] A. V. Grigorieva[a,*], A. V. Sidorov[a], A. Yu. Polyakov[a], I. V. Sukhorukova[b], D. V. Shtansky[b], W. Grünert[c], and E. A. Goodilin[a]

Pristine and artificially mixed silver colloids of diverse anisotropic silver nanoparticles were used as “rainbow” colloidal silver inks for inkjet printing of cellulose-based active elements with polychromatic sensitivity for Surface-Enhanced Raman Spectroscopy optical sensors. Platelete silver nanocrystallites possessing different plasmonic bands in the visual spectral range were grown up in water-polyol liquors of different viscosities to prevent nanoparticle agglomeration and provide colloidal stability for at least one year. SERS tests of model photostable dyes revealed bright enhanced signals under several standard wavelengths of laser irradiations thus demonstrating better practical applications of such substrates.

Introduction

Silver colloids are highly important materials for biomedicine, electrochemistry, microelectronics, heterogeneous catalysis and photocatalysis, advanced energy storage and ecology purposes although it is surface enhanced Raman spectroscopy (SERS) phenomenon that makes them of special interest for practical applications as promising optical sensors.[1] Most of these numerous applications are, in fact, dependent on the surface state of silver nanoparticles while their micromorphology is one of the key factors which limit or improve their functional characteristics.

Both colloidal silver and gold are of greater interest among all other metals because their surface plasmon bands are quite strong and belong to the visible range. The shape and anisotropy of nanoparticles are then the key features which modulate plasmon extinction spectra of both the metal colloids and their nanocomposites. Nowadays, a number of synthetic approaches are well-optimized to yield reproducibly surfactant - stabilized sols of round-shaped particles,[2,3] nanorods[4], nanocubic,[5-7] cage-like structures and hollow polygrans,[8-11] plate-like,[12,13] triangular[14,15], or star-like nanoparticles.[16] Nevertheless, the synthesis of stable plasmon multicolored colloids with a desired shift of plasmon maxima is still a challenge. As compared with physical routes of silver nanoparticles processing, such as magnetron sputtering or ion implantation, soft chemical methods are more successful in producing uniform and narrow sized distribution of polyhedral nanoparticles with multiple surface plasmon resonance modes.

As known for decades[17], silver hydrosols are effective plasmon materials in the visible range extremely promising for the SERS technique. Nowadays, an undeniable fact is that SERS-active substrates allow for detecting of nanomole or even femptomole concentrations of organic species like dyes, medicals, biomolecules or drugs, taggants, etc.[2,18-21] An ability to shift or expand plasmon maxima to tune the triple “laser-plasmon-analyte” system is mostly feasible via varying shapes and sizes of individual nanoparticles or making their aggregates. Stable colloids are easy-to-work-with materials allowing almost full control of the additive plasmon spectra by using standard inexpensive preparation procedures.[14] Most colloids, including those which demonstrate the Tyndall effect, are combining easily giving an additive absorption spectra.[3] Therefore, stable “rainbow” mixed silver colloids are of great interest for a modern SERS analysis.

Ink jet printing is a promising technique to produce large planar or 3D structures combining individual nanoparticles as the smallest element of outcome microstructures and the “coffee ring” motif as a secondary surface relief element.[20] Several chemical preparation approaches for Ag colloidal inks are described.[3,19,22] As reported by Kim et al.[22] viscosity of inks for inkjet printers varies in the range of 2.5 – 5.6 mPa·s while the surface tension is usually about 40 mN/m. Successful inkjet printing of conductive circuits requires high concentration of silver in the printer ink, not less than 10^{-4} M, to accomplish deposition in a reasonable number of printing cycles followed by removing of non-volatile compounds by annealing of the substrates in air at 100 – 300°C for 0.5 – 2 h.[22] In particular, centrifugation is known as a helpful method to concentrate colloidal silver and optimize the overall printing process.[19] In the case of SERS-active substrates, the printing process

---

[a] *Department of Materials Science, Lomonosov Moscow State University, Leninskie gory 1, bld. 73, Moscow 119991, Russia*
[b] *National University of Science and Technology “MISiS, Leninsky prospect 4, Moscow 119049, Russia*
[c] *Department of Chemistry and Biochemistry, Ruhr-University at Bochum, Universitatsstrasse 150, Bochum 44801, Germany*
* Corresponding author, anastasia.grigorieva@gmail.com, +7 (495) 939 09 98 (fax)

Electronic Supplementary Information (ESI) available: [supplementary figures]. See DOI: 10.1039/x0xx00000x becomes easier since it is not demanded to achieve the formation of highly percolating clusters therefore concentrations of metal nanoparticles should not be high and thus neither preconcentration nor annealing are necessary procedures. This expands also the number of suitable substrates to deposit the silver nanoparticle sols.

Here, we synthesized silver rainbow inks via a two-step process involving water, water – ethylene glycol (H_2O–EG) or water – glycerol (H_2O–GL) liquors. An optimal viscosity of inks (*1.5 – 2.0 cSt*) was achieved (ESI, Table S1). Substrates of various sizes including single active elements of SERS sensors as small as 1 mm^2 were successfully inkjet printed using the prepared silver sols, and then their SERS activity and polychromatic sensitivity were demonstrated.

Experimental

Synthetic procedures and inkjet printing

Silver nitrate (≥ 99 % , Ph.Eur., extra pure) was purchased from Carl Roth GmbH. Sodium borohydride (granular ≥98%) was purchased from Aldrich. Sodium citrate (tribasic dihydrate, p.a., ACS reagent, ≥99.0%) was purchased from Sigma-Aldrich. Polyvinylpyrrolidone (PVP, K30, extra pure, M_w~40 000) was purchased from Carl Roth. All other reagents and solvents were of an analytical grade. Purified water (MilliQ) was used for aqueous solutions preparation. All glassware was rinsed with concentrated HNO_3 before the syntheses.

Silver plate-like particles were synthesized via a standard two-step process[23]. For the first, silver seeds of about 8-10 nm in diameter were obtained as a primary colloidal reagent by using of the standard reduction of silver nitrate by sodium borohydride in the presence of sodium citrate. For that, 220 ml of 10^{-4} M $AgNO_3$ and $2{\cdot}10^{-3}$ M of sodium citrate solution was rapidly mixed with freshly prepared 6 ml of $5{\cdot}10^{-3}$ M $NaBH_4$ solution under vigorous stirring. To visualize the end of the process, 5 ml aliquotes were taken every 5 - 10 min during 30 minutes. Large SERS-inactive particles and aggregates could be removed from the liquor using the syringe driven filter unit (Millex® - HV) with a pore diameter of 0.45 µm. The overall concentration of silver in the primary colloid was still about 10^{-4} M, so that an estimate percentage of nanoparticles in the resulting colloid was about $3.3{\cdot}10^{23}$ particles per liter.

For the synthesis of plate-like particles, the primary round-shaped colloidal particles served as the seeds in heterogeneous growth of the crystallites. PVP was a stabilizer and the ascorbic acid served as an effective reducing substance. Namely, 5 ml of $5{\cdot}10^{-3}$ M $AgNO_3$, 15 ml of $3{\cdot}10^{-2}$ M sodium citrate and 15 ml of $7{\cdot}10^{-4}$ M of PVP is dissolved in 125 ml of water or in different ethylene glycol-water or glycerol-water solutions. Then different water aliquotes of seeds were added under stirring for 20 min to spread the silver seeds and provide their uniform growth. The taken aliquots were of the following volumes: 3.2 ml, 9.6 ml, 12.8 ml, 19.2 ml, 22.0 ml, 25.6 ml, 51.2 ml, 76.8 ml, 153.6 ml and 384.0 ml. Finally, 125 ml of 10^{-3} M aqueous solution of ascorbic acid was injected rapidly under vigorous stirring. Immediately after that, colloids become colored; the color did not show changes already after 15 min of the reaction. For the “rainbow silver inks” the concentration of silver increased slowly in the range of $0.88{\cdot}10^{-4}$ – $0.95{\cdot}10^{-4}$ M as proportional to the volume of silver seeds injected.

The same procedures were repeated in water – ethylene glycol (H_2O–EG) or water – glycerol (H_2O–GL) liquors. Different H_2O/EG and H_2O/GL molar ratios were used to vary hydrodynamic viscosity and prevent aggregation of the final colloids. An Epson Workforce 30 inkjet printer was chosen to generate the SERS-active substrates. Epson’s Micro Piezo technology uses piezo elements to propel ink onto the substrate, in contrast to the thermal method which uses heat to create air bubble. Piezo elements are much more appropriate for different kinds of reagents used for printing.

Analytical Methods

The colloids were characterized by transmission electron microscopy (TEM) combined with electron diffraction (ED) using a LEO 912 AB OMEGA microscope (Carl Zeiss) at 100 kV accelerating voltage. Diameters or linear sizes of about two hundred of nanoparticles in TEM images were measured for a statistical analysis of the particles. The Gauss function was applied for the estimation of mean diameters and standard deviations.

UV-vis absorption spectra were recorded using a UV-vis spectrometer Lambda 950 (Perkin-Elmer) with an attached diffuse reflectance accessory. Measurements were performed in the range of 250 - 850 nm with a scanning rate of 2 nm/s.

Hydrodynamic radii of particles or their aggregates were analysed by the dynamic light scattering (DLS) technique using a Malvern Zetasizer Nano ZS instrument at 25°C with a He–Ne laser (laser power: 4 mW, wavelength: 632.8 nm, beam diameter: 0.63 nm). The scattering and detection angles were 175 and 12.8°, respectively. The estimates of relative amounts of nanoparticles (ESI, Table S1) were calculated as a ratio of DLS peak areas corresponding to small and large characteristic measures.

Measurements of kinematic viscosity were performed using an Oswald-type glass capillary viscometer at 25°C. The capillary diameter was 131 mm. Kinematic viscosity was calculated according to the equation $V=g{\cdot}t{\cdot}K/9.807$, where V is kinematic viscosity (mm^2/s), K is a viscometer constant of 0.277 mm^2/s^2, t – a liquid outflow time per second, g – the gravitational acceleration in m/s^2, and 9.807 m^2/s is a constant.

SERS experiments were performed using an InVia Raman confocal microscope setup (Renishaw Inc.) equipped with a 20 mW 514.4 nm argon laser and power neutral density filter (1-10%) and a 20 mW 632.8 nm Ne-He laser. All the spectra were collected with 10 s of acquisition time using a confocal microscope Leica DMLM (resolution up to 2.5 µm) equipped with 20x and 50x objective lens. Diffraction grating was 2400 lines/mm, CCD camera 1024 x 256 pixels. A silicon wafer was used for calibration. The aliquot volume of analytes was 10 µl.

X-ray photoelectron spectroscopy was performed using the setup ESCA I at the laboratory of industrial chemistry at RUB. The X-ray source was Specs XRC 1000, and the energy analyzer

- PS-EA10N. Pre-vacuum pressure gauge (Leybold Thermovac TM20) with the pressure of up to 10^{-3} mbar; UHV-chamber gauges provided up to $1{\cdot}10^{-8}$ mbar pressure. Metallic gold served for the calibration. UNIFIT software was applied for XPS profile analysis. NIST XPS database files served as references.

Results and discussion

Silver rainbow ink preparation includes an application of small Ag seeds (9±2 nm diameter) as heterogeneous nuclei for Ag platelets growth (Fig.1). Different Ag seed aliquots were used to study their effect on the final colloid formation. Increasing the Ag seed aliquote volume in the second step of the synthesis we decrease significantly the $AgNO_3$/Ag-seed concentration ratio and it results in growth of anisotropic silver nanoparticles of different sizes and shapes (Fig. 1). The electron diffraction of larger silver particles (sample “12.8”) (Fig. 1c) evidences for the cubic phase of metallic silver while for smaller particles of 9 nm in lateral size (sample “76.8”) it looks amorphous. According to the XPS data, a valent state of the silver particles fits well the metallic Ag^0 state with two binding energies of Ag $3d_{5/2}$ and Ag $3d_{3/2}$ at 366.0 eV and 372.0 eV, respectively. For silver nanoparticles stabilized by PVP or citrate molecules this indicates that the surface states of silver are rather similar to an unmodified metal.

It is observed that the dynamic viscosity η of silver colloids depends not only on liquid phase composition but also on particles micromorphology decreasing with a lateral size decrease (Fig. 2a, Table S1). A variation of preparation parameters controls the plasmon resonance spectra of both the inks and the related planar structure.

Absorption spectra of the hydrosols manifest this method as an efficient one to manipulate plasmon bands accurately (Fig. 2b). Most of the spectra have three or four evident maxima which, most likely, correspond to a mixture of round shaped particles[3] or triangular prisms[13] or both. Both TEM (Fig. 1) and DLS data (Fig. S2) correlate well with the purpose above confirming the presence of both round-shaped particles together with triangular and disc-like particles. Graphical representation of characteristic particle size for different liquors is given in Fig. 1h and Table S1 (ESI).

In general, the correlations found out agrees with the results reported by D. Jana and G. De;[5] the authors declare a red shift for the largest plasmon peak with an increase of silver particles being nucleated directly on alumina sol. Our findings confirm that the silver crystal growth in the (111) plane correlates with the red shift of a broad plasmon peak. In this study, the red color of silver colloids alternated with the particle size decrease by purple, purple by marine blue and, finally, the blue turns into cyan and then emerald green (Fig. 2b). Stability of the hydrosols with time was analyzed using UV-vis spectrometry and confirms that keeping of the hydrosols at 4°C for 6 months resulted in a particle size decrease (green turned cyan, blue turned purple and red, red turned orange) contrary to the Ostwald growth process (see Fig. 3c).

To prevent aggregation of nanoparticles during sedimentation and solvent exchange procedure, the synthesis of SERS-active inks was performed directly in more viscous water-polyol media, lowering at the same time the particle growth rate and preventing side nucleation process (Table S1). The colloids produced were examined as model nanoinks for inkjet printing.

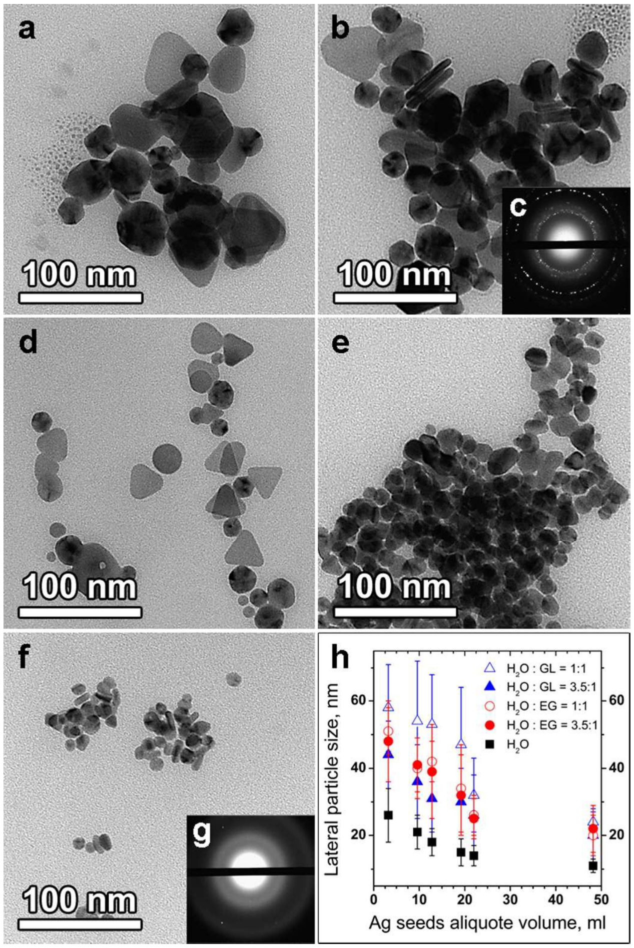

Fig. 1. TEM data of silver hydrosols synthesized with different aliquots of seeds of (a) 3.2 ml; (b) 12.8 ml, SAED is given in the (c) inset; (d) 25.6 ml, (e) 51.2 ml, (f) 76.8 ml, SAED is given in (g). (h) graphical representation of the particle size changes with Ag seeds aliquote volume in aqueous, H_2O-EG and H_2O-GL media.

By the same way as rainbow hydrosols, water-polyol silver colloids changed their color from green to yellow depending on an aliquote of Ag seed used in the synthesis. According to TEM statistics, silver crystals vary their lateral size (*L*) within a wider range in the case of water-polyol media as compared to hydrosols (Fig. 1h). The *L* value falls evenly with a linear increase of the volume of Ag seed aliquote for all the four compositions of the H_2O–EG and H_2O–GL liquors. It is remarkable that the *L* value in either the H_2O–EG or H_2O–GL liquors surpasses more than twice the hydrosol particle sizes grown up with similar precursor ratios.

The 77.5% H_2O – 22.5% EG and 77.5% H_2O – 22.5% GL colloids are quite identical to those prepared in water media but all the absorption spectral maxima are wider. The overall intensities of the UV-Vis absorption spectra are smaller than those for hydrosols that, likely, correlates with the particle concentrations in the inks (Fig. 2b-f). The same works for liquors of higher polyol content, especially for the 50% H_2O – 50% GL media (Fig. 2f). In contrast with ethylene glycol, glycerol does not reduce silver nitrate even on heating up to 90°C, thus being a more inert solvent of higher redox potential at standard temperature[24] This is to support that the secondary nucleation takes place in hydrosols and, probably, in H_2O–EG mixtures. A blank experiment, however, shows a quite weak reduction activity of ethylene glycol at room temperature but rapid formation of silver particles after ascorbic acid injection. Most likely, a lower diffusion rate of the reducing agent (ascorbic acid) limits the secondary nucleation process through this increasing the particle size (Fig. 2a). As soon as silver particles grow up in the (111) plane, while (111) direction is substantially blocked by PVP molecules, the lateral particle size increases significantly changing the wavelengths of plasmon vibrations.

The increase of the *L* value was accompanied by a red shift of the plasmon peak (Fig. 2c-f) similar to that observed for silver hydrosols. UV-vis spectra for 77.5% H_2O – 22.5% EG and 77.5% H_2O – 22.5% GL compositions correlate better with corresponding hydrosols by color while the maximum at around 400 nm is much less intensive than for hydrosols. The 50/50 compositions, being more viscous, extend the crystal growth process in time thus preventing the secondary nucleation process and leading then to green and blue-colored colloids. A high content of silver seeds in 50/50 liquors results in red-colored inks. In contrast to hydrosols, the rainbow colloids of higher viscosity showed an excellent stability and reproducibility of absorption spectra for over a year.

The most important advantage of inkjet printing for SERS detecting systems (Fig. 3a-d) is the ability to use one small probe of 10 µl or less to analyze desired analytes at multiple points at once with an enhancement factor of up to 10^6. Citrate and PVP form standard adsorbate coverage over silver nanoparticles providing similar adsorption properties of different areas of the substrate. Rhodamine 6G was chosen as a model analyte for SERS experiments because of its known photostability.[25] Concentrations of Rhodamine 6G in our Raman experiments were as small as 10^{-6} M and 10^{-7} M; that is enough to demonstrate the SERS effect while no signal from the dye is observed without plasmon structures under standard setup settings. The measurement was performed using 514.4 nm and 632.8 nm lasers to compare preresonant and non-resonant Raman measurements. According to Fig. 3 the SERS signal intensity is similar for most of rainbow hydrosols with various plasmon resonance maxima positions, but less intensive for green-colored (largest) silver particles.

The Nano-inks based on 50% H_2O – 50% EG compositions were used in inkjet printing experiments because of the most appropriate viscosity values. As anticipated, all the printed inks feature out SERS spectra of Rhodamine 6G (Fig. 3e). Unlike purple-red-colored inks, both green (3.2 ml and 9.6 ml of seed aliquote) and blue (19.2 ml seed aliquote) inks did not show any SERS-spectra appropriate for further analysis neither with 514.4 nm lasing nor with 632.8 nm excitation.

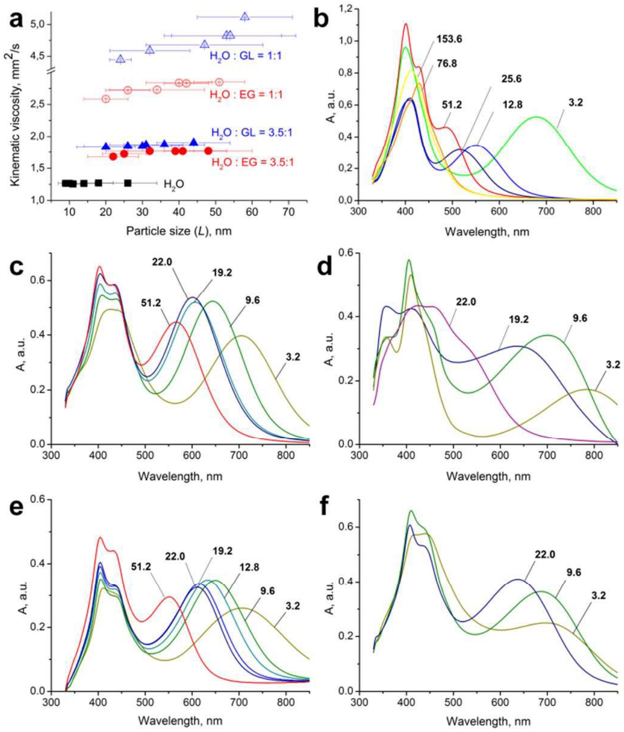

Fig. 2. Characteristics of silver inks. (a) Kinematic viscosity against a mean particle size (TEM data). UV-vis spectra of silver hydrosols and inks prepared in different liquors: (b) H_2O, (c) H_2O : EG = 3.5:1, (d) H_2O : EG = 1:1, (e) H_2O : GL = 3.5: 1, (f) H_2O : GL = 1:1. The volumes of Ag seed aliquots (in ml) used in the sample syntheses are the labelling.

An amazing analogy with spectral characteristics of rainbow inks is observed as an important strong morphology-to-SERS effect correlation (Fig. 3e, 2d). Under the 514.4 nm laser excitation, the least effective printed areas in Rhodamine 6G detecting correspond to the smallest Ag particles (yellow-colored) and the largest ones (green-colored). Most probably, the small effect is due to a low absorption of 514.4 nm laser irradiation by green-colored colloid that excludes a ternary coinciding effect of “laser wavelength - surface plasmon band – molecule absorption”. A stronger effect is observed in the case of blue and purple nanoinks when more intense extinction at the 514 nm wavelength takes place.

In the case of the purple - red gamma of the inks, the deposited Rhodamine 6G shows relatively good SERS spectra for both the 10^{-6} and 10^{-7} M concentrations (Fig. 3e). The most intense Raman modes at 1365, 1508 and 1645 cm^{-1} should be associated with C-C stretching bands of the Rhodamine 6G aromatic skeleton.[26] In the most of cases, SERS intensity values are appropriate for detecting of the model analyte at standard concentrations of ca. 10^{-6} M while the enhancement factor $G = I_{SERS} \cdot c_R / I_R \cdot c_{SERS}$ is ~ 10^4 (c_{SERS} and c_R are Rhodamine 6G concentrations in aliquots and I_{SERS} and I_R are Raman signal intensities of the 1508 cm^{-1} mode in corresponding spectra).

Switching to the 632.8 nm red laser yields in SERS spectra with a less intense background signal originating from fluorescence of cellulose and the analyte. The spectra of Rhodamine 6G deposited onto inkjet modified filter paper do not reveal any strong Raman mode of the dye. At the same time Raman spectra of the samples contain intensive vibration modes of the cellulose which serves as a flexible substrate for the nanoparticles. Fig S3 (ESI) demonstrates the SERS spectra of bare filter paper wafer[27] which differ in most intensive characteristic modes with cellulose Raman spectra.[27] Compared to the Raman data of De Gelder et al.,[27] cellulose vibration modes at 436(s), 459(s), 1155(s), 1339(s), and 1379(s) cm^{-1} are intensified in the SERS spectra observed.

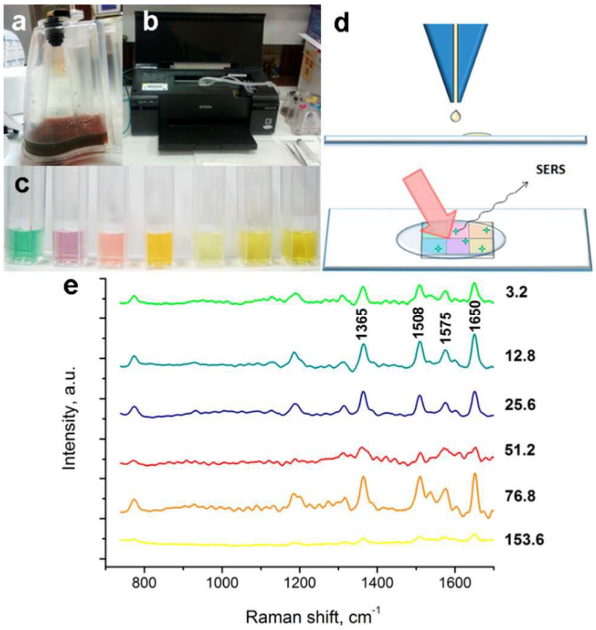

Fig. 3. A view of the inkJet printing system to generate the SERS-active substrates. (a) NanoInk of silver colloid, (b) Commercial inkjet printer Epson Workforce 30, (c) Silver Nano-Inks with particles of various sizes and shapes. (d) A principal scheme of the experiment (e) SERS spectra of Rhodamine 6G of 10^{-7} M concentration (10 µl aliquote) taken using ash-free filter paper with the inkjet printed rainbow sols (514.4 nm Ar laser, 1% of 14 mW; 10 s exposition; single crystalline Si (100) as a standard for calibration).

The features of Raman enhancement with water-polyol compositions deals with not only impaired kinetics of crystal growth but also with long evaporation of the solvent at standard temperature. Otherwise, heating is able to initiate Ag$^+$ ion reduction with polyol molecules (with EG already at 70°C) and to change spectral characteristics of the colloids. Glycerol is steadier to be evaporated but is more appropriate as a natural biocompatible polyol for living cells analysis.

Conclusions

Successful inkjet printing of SERS-active silver nanoinks on paper-based substrates as small as 1 mm^2 are of substantial demand for forensic, medical and health care everyday purposes as multifunctional SERS-active microsensors in prospect. The rainbow nano-inks of 1.5-2.0 cSt could be printed and then be used for analysis. Advantage of mixed-solvent inks deals also with improved stability of the colloids in time, while nucleation and the Ostwald growth of the silver is surpassed.

Acknowledgements

Authors are grateful to Prof. Yuri V. Traskine and Aksana M. Parfenova (Colloid Chemistry Division), who initiated effective collaboration of two divisions; students Valery A. Bannikova, Vlad D. Chernyshov, Elya A. Tastekova, Gleb Yu. Alyoshin for their experimental assistance. The international cooperation of the MSU and RUB was supported by grants of the Leonhard-Euler-Program of Deutscher Akademischer Aushtausch Dienst (DAAD). This project is financially supported by the Russian Foundation of Basic Research (grants 13-03-12190-ofi_m, 13-03-01143-a, 15-33-70050-mol_a_mos). The authors gratefully acknowledge the financial support of the Ministry of Education and Science of the Russian Federation in the framework of Increase Competitiveness Program of MISiS (Agreement #02.A03.21.0004 of 27.08.2013).

Notes and references

1 Q.H. Tran, V.Q. Nguyen and A.-T. Le, *Adv. Nat. Sci.: Nanosci. Nanotechnol.*, 2013, **4**, 033001-1-033001-20
2 A.M. Michaels, M. Nirmal and L.E. Brus, *J. Am. Chem. Soc.*, 1999, **121**, 9932.
3 T. Huang and X.-H. N. Xu, *J. Mater. Chem.*, 2010, **20**, 9867.
4 A. Jakab, C. Rosman, Y. Khalavka, J. Becker, A. Trügler, U. Hohenester and C. Sönnichsen. *ACS Nano*, 2011, **5**, 6880.
5 D. Jana and G. De, *J. Mater. Chem.*, 2011, **21**, 6072.
6 M.A. Mahmoud, C.E. Tabor and M.A. El-Sayed, *J. Phys. Chem. C*, 2009, **113**, 5493.
7 A. Moreau, C. Ciracì, J.J. Mock, R.T. Hill, Q. Wang, B.J. Wiley, A. Chilkoti and D.R. Smith, *Nature*, 2012, **492**, 86.
8 L. Au, Y. Chen, F. Zhou, P.H.C. Camargo, B. Lim, Z.-Y. Li, D.S. Ginger and Y. Xia, *Nano Res.*, 2008, **1**, 441.
9 S.E. Skrabalak, J. Chen, Y. Sun, X. Lu, L. Au, C.M. Cobley and Y. Xia, *Acc. Chem. Res.*, 2008, **41**, 1587.
10 Z. Zhang, Y. Chen, X. Xu, J. Zhang, G. Xiang, W. He and X. Wang, *Angew. Chem. Int. Ed.*, 2014, **53**, 429.
11 M. Tsuji, T. Kidera, A. Yajima, M. Hamasaki, M. Hattori, T. Tsuji and H. Kawazumi, *Cryst. Eng. Comm.*, 2014, **16**, 2684.
12 Z. Li, G. Meng, T. Liang, Z. Zhang and X. Zhu, *Applied Surface Science*, 2013, **264**, 383.
13 L.J. Sherry, R. Jin, C.A. Mirkin, G.C. Schatz and R.P. Van Duyne, *Nano Lett.*, 2006, **6**, 2060.
14 G. Si, W. Shi, K. Li and Z. Ma. *Eng. Aspects*, 2011, **380**, 257.
15 L. Xu, Z. Luo, Z. Fan, X. Zhang, C. Tan, H. Li, H. Zhang and C. Xue. *Nanoscale*, 2014, **6**, 11738.
16 J.M. Köhler, H. Romanus, U. Hübner and J. Wagner, *J. Nanomaterials*, 2007, Article ID 98134.
17 M. Moskovits, *Phys. Chem. Chem. Phys.*, 2013, **15**, 5301.
18 C. Andreou, M.R. Hoonejani, M.R. Barmi, M. Moskovits and C.D. Meinhart, *ACS Nano*, 2013, **7**, 7157.
19 W.W. Yu and I.M. White, *Analyst*, 2013, **138**, 3679.
20 A.S. Sarycheva, A.A. Semenova, E.Y. Parshina, N.A. Brazhe, A.Yu. Polyakov, A.Y. Kozmenkova, A.V. Grigorieva, G.V. Maksimov and E.A. Goodilin, *Mater. Lett.*, 2014, **121**, 66-69
21 R.D. Deegan, O. Bakajin, T.F. Dupont, G. Huber, S.R. Nagel and T.A. Witten, *Nature*, 1997, **389**, 827.
22 D. Kim, S. Jeong, B.K. Park and J. Moon, *Appl. Phys. Lett.*, 2006, **89**, 264101.

23 Yu. D. Tretyakov, E. A. Goodilin, *Russian Chemical Reviews*, 2009, **78** (9), 801-820.
24 H. Adkins, R.M. Elofson, A.G. Rossow and C.C. Robinson, *J. Am. Chem. Soc.*, 1949, **71**, 3622.
25 I. Rosenthal, *Optics Commun.*, 1978, **24**, 164.
26 S. Nie and S.R. Emory, 1997, **275**, 1102.
27 J. De Gelder, K. De Gussem, P. Vandenabeele and L. Moen, *J. Raman Spectrosc.*, 2007, **38**, 1133.

Inkjet Printing of Silver Rainbow Colloids for SERS Chips with Polychromatic Sensitivity

K. E. Yorov,[a] A. V. Grigorieva[a,*], A. V. Sidorov[a], A. Yu. Polyakov[a], I. V. Sukhorukova[b], D. V. Shtansky[b], W. Grünert[c], and E. A. Goodilin[a]

Graphical Abstract

Polychromatic cellulose-based active element for SERS optical sensor was successfully inkjet printed using pristine and artificially mixed silver colloids as the inks. Different kinds of silver platelet nanocrystallites possessing different plasmonic bands in the visual spectral range were synthesized directly in water-polyol liquors of different viscosities to provide high colloidal stability. SERS tests of model photostable analytes revealed most bright enhanced signals for the cases of preresonant measurements.